Influence of organic ligands on the line shape of the Kondo resonance

Jörg Meyer, Robin Ohmann, Anja Nickel, Cormac Toher, Roland Gresser, Karl Leo, Dmitry A. Ryndyk, Francesca Moresco, and Gianaurelio Cuniberti

Phys. Rev. B **93**, 155118 — Published 12 April 2016

DOI: 10.1103/PhysRevB.93.155118

Influence of organic ligands on the line shape of the Kondo resonance

Jörg Meyer,[1,2] Robin Ohmann,[1] Anja Nickel,[1,2] Cormac Toher,[1] Roland Gresser,[3] Karl Leo,[3,2] Dmitry A. Ryndyk,[1,2] Francesca Moresco,[1,2] and Gianaurelio Cuniberti[1,2,4]

[1]*Institute for Materials Science and Max Bergmann Center of Biomaterials, TU Dresden, 01062 Dresden, Germany*

[2]*Center for Advancing Electronics Dresden, TU Dresden, 01062 Dresden, Germany*

[3]*Institut für Angewandte Photophysik (IAPP), Technische Universität Dresden, 01062 Dresden, Germany*

[4]*Dresden Center for Computational Materials Science (DCMS), TU Dresden, 01062 Dresden, Germany*

Abstract

The Kondo resonance of an organic molecule containing a Co atom is investigated by scanning tunneling spectroscopy and *ab-initio* calculations on a Ag(100) surface. High resolution mapping of the line shape shows evidence of local non-radially symmetric variations of the Fano factor and the Kondo amplitude, revealing a strong influence of the molecular ligand. We show that the decay of the amplitude of the Kondo resonance is determined by the spatial distribution of the ligand's orbital being hybridized with the singly occupied Co d_{z^2} orbital, forming together the singly occupied Kondo-active orbital.

PACS numbers: 72.15.Qm, 68.37.Ef, 71.15.Mb

Understanding the influence of the ligands on the magnetic properties of single metal atoms incorporated in organic molecules is of crucial importance for the development of molecular electronics and spintronics. In the past years, an increasing number of molecular systems showing a Kondo resonance have been investigated [1–8]. The Kondo resonance is known to be caused by spin-flip scattering of electrons on magnetic impurities in a non-magnetic host. It can even be observed in molecular systems which do not possess magnetic atoms but have a single spin in one of the molecular orbitals [3, 5]. In other molecular systems, the atomic levels of the magnetic atom are strongly hybridized with the organic ligand, leading to a stronger spatial spreading of molecular orbitals originating from the d- or f-states of the magnetic atoms compared to atomic Kondo impurities [1]. The combination of organic ligands with magnetic atoms creates a great opportunity to investigate and engineer the interaction and assembly of magnetic atoms to form Kondo lattices [9], which may lead to new heavy fermion materials or Kondo insulators. Since more than 15 years, scanning tunneling spectroscopy (STS) is an established experimental technique to investigate the Kondo resonance with high spatial resolution [10, 11]. While there are several examples of single atoms showing a radially symmetric distribution of the Kondo resonance [12–14], investigations on the propagation of the Kondo resonance within an organic ligand are rare. To our knowledge, a high resolution mapping of the Fano factor q has not been reported so far. This is, however, one of the key parameters defining the line shape of the Kondo resonance and hence the low-bias conductivity of the molecule.

In this article, we present the results of spatially resolved STS experiments on single organic molecules with a central Co atom on Ag(100). We show the large spatial extent of the Kondo resonance (compared to atomic Co) and its dependence on the electronic structure of the organic ligand. The influence of the organic ligand is studied by density functional theory (DFT) calculations of the Co d-state hybridized with the states of the organic ligand and the metal surface. We report a change in the symmetry of the Kondo resonance between different points on the same molecule (without altering its structure like in [4]). This change in symmetry is evidenced by the changing sign of the asymmetry factor q in the Fano function. From a grid of spectra over the molecule, we obtain spatial maps of the fitting parameters for the Kondo resonance with sub-molecular accuracy.

The measurements shown here were performed by scanning tunneling microscopy (STM) at low temperatures (T=5 K) and a base pressure below 10^{-10} mbar. The Ag(100)

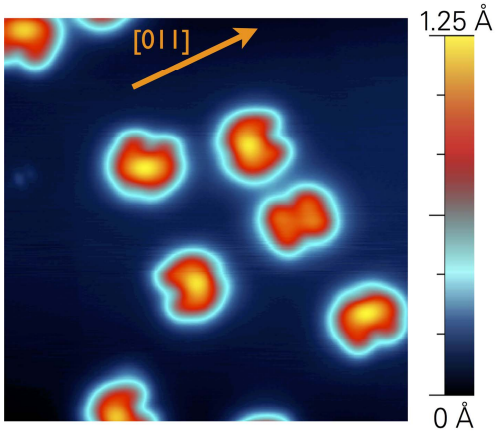

FIG. 1. (Color online) Overview STM image of Co-BiPADI and BiPADI on Ag(100): The Co atoms in Co-BiPADI can be seen as central protrusions (yellow). Adsorbates without this protrusion are BiPADI and do not show any Kondo resonance. The Ag crystal orientation was deduced from the orientation of the step edges and is marked with the orange arrow (image size 100 Å x 100 Å).

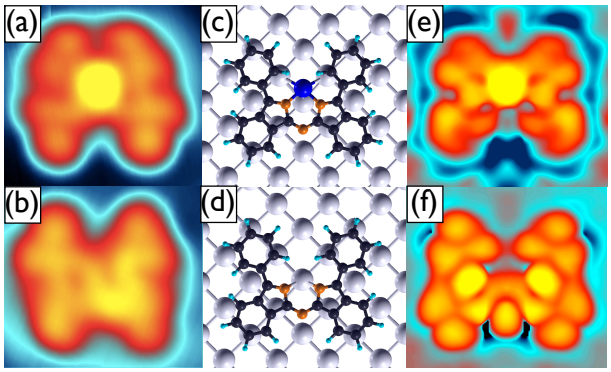

FIG. 2. (Color online) STM images and DFT calculations of the two fragments of Co-$(BiPADI)_2$ on Ag(100). (a) STM image of the fragment containing Co and attributed to Co-BiPADI; (b) STM image of the fragment without Co, attributed to BiPADI (a,b; image size 20 Å x 17 Å, V_b = -0.1 V, I_t = 1 nA); (c) calculated structure of Co-BiPADI on Ag(100); (d) calculated structure of BiPADI on Ag(100); (e,f) simulated STM images corresponding to (c) and (d), respectively (image size 16 Å x 15 Å). Color code for panels (c) and (d): Ag=gray, C=black, H=light blue, N=light brown, Co=dark blue.

surface was cleaned by several cycles of sputtering and annealing. Co-di-bis-(phenyl)-azadiisoindomethene (Co-$(BiPADI)_2$) was evaporated at submonolayer coverage from a Knudsen cell at 160 °C onto the metal sample kept at room temperature. On the surface,

two types of molecular adsorbates were observed by STM (Fig. 1), indicating that the compound decomposes in two fragments during sublimation. The structure of those two different adsorbates was verified by DFT calculations. From Fig. 1 it is clear that we observe at least two symmetrically equivalent orientations of Co-BiPADI on Ag(100). One orientation is parallel to the (011) direction and its symmetry equivalents, the other orientation is inclined to this direction by about 15^o. Both orientations have been confirmed by calculations but no significant spectroscopic difference was detected. The STM images of the two adsorbates are compared to DFT calculations in Fig. 2. The simulated STM images were generated using spin-polarized DFT calculations with the local spin density approximation (LSDA) to the exchange correlation potential. The calculations were performed using SIESTA [15] with a 4 x 4 x 1 Monkhorst-Pack k-point grid. The basis set was constructed using a 0.002Ry energy shift to set the cut-off radii, with double zeta 3d, 4s and 4d orbitals for the Co atom, double zeta 2s and 2p orbitals for the C and N atoms, double zeta 1s orbitals for the H atoms, and double zeta 4d and single zeta 5s and 5p atoms for the Ag atoms. The geometry optimization calculations were performed using a slab 3 Ag layers thick, where the topmost atomic Ag layer and all of the atoms of the Co-BiPADI molecule were allowed to relax in order to reduce the forces below a threshold of $0.05\text{eV}/\mathring{A}$. The excellent agreement between the experimental and simulated images let us assign the two fragments to Co-bis-(phenyl)-azadiisoindomethene (Co-BiPADI)) (Fig. 2(a,c,e)) and bis-(phenyl)-azadiisoindomethene (BiPADI) (Fig. 2(b,d,f)). The decomposition of Co-$(\text{BiPADI})_2$ into Co-BiPADI and BiPADI give us the unique opportunity to investigate the same organic molecule with and without a central Kondo impurity, simultaneously and under the same experimental conditions.

In Fig. 3(a), a STS spectrum of the Co atom incorporated into the organic ligand is shown and compared to the spectrum of the isolated organic ligand. On Co-BiPADI, a pronounced peak at the Fermi energy is observed, while for the bare organic ligand no peak is measured at this energy. The peak is ascribed to the Kondo resonance and will be explained in detail below. Furthermore, a broad less intense peak is observed at $V_{bias} \approx$ -80 mV, which is present on both molecules with and without the Co atom and is ascribed to a molecular resonance.

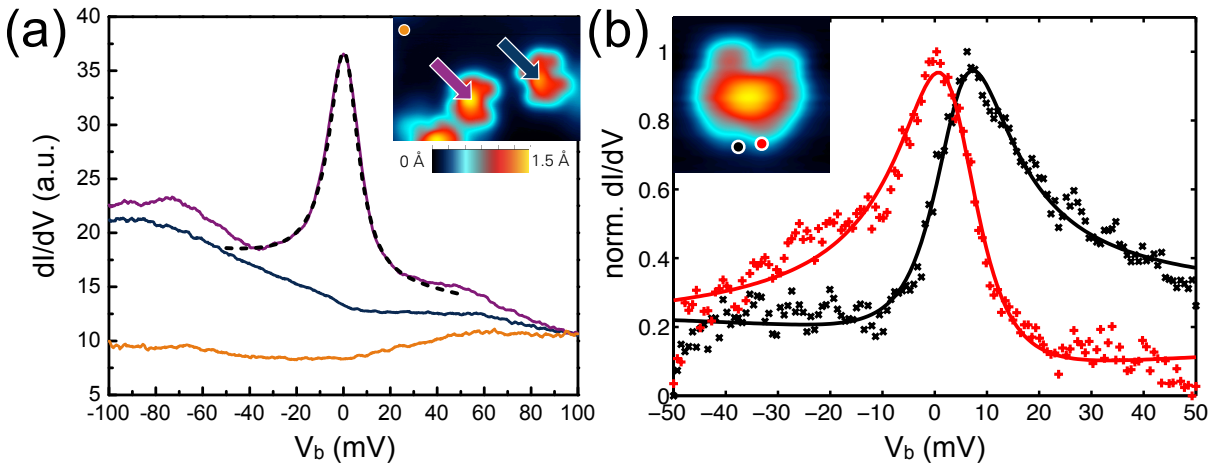

FIG. 3. (Color online)(a) dI/dV spectra of Co-BiPADI (violet), BiPADI (blue) and the bare Ag surface (orange). The Fano fit of the Kondo resonance on Co-BiPADI is given as a dashed black line; (b) normalized dI/dV spectra with positive (black +) and negative (red x) q factors with corresponding fits (solid lines, q factor 2.4 (black) and -3.6 (red)). The inset shows STS positions (image size (a) 61 Å x 25 Å, (b) 25 Å x 25 Å).

The observed Kondo peak was fitted with a Fano function:

$$\frac{dI}{dV} = a\frac{(q+\epsilon)^2}{1+\epsilon^2} + bV_b + c;\ \epsilon = \frac{eV_b - E_0}{k_B T_K} \tag{1}$$

where E_0 is the energy shift, $k_B T_K$ the half width at half maximum at T=0 and q the asymmetry or Fano factor. The equation is valid for a single-level model, at low-temperatures and small voltages [10, 16]. Background subtraction was performed according to the formalism by Wahl *et al.* [17] and the linear term b takes into account the ligand states influence in the spectroscopic region of interest ($V_{bias} = \pm$ 50 mV). The line shape at the center of the molecule was fitted with the following parameters, the values for atomic Co on Ag(100), taken from ref. [18] are given in brackets for comparison: $k_B T_K$ = 8.44 meV leading to a Kondo temperature of T_K = 98.0 K ([18]: T_K = 41 K). The energy shift yields E_0 = 0.71 meV ([18]: E_0 = 2.0 meV) and the asymmetry factor on top of the Co atom is q = -15.9 ([18]: $q \approx 0$).

Furthermore, we also performed STS measurements at increased substrate temperature to verify the Kondo-nature of the resonance. The temperature dependence of the half width at half maximum (HWHM) of the Kondo resonance is shown in Fig. 4. Due to the flat DOS of tip and substrate near the Fermi level, the influence of background subtraction on the

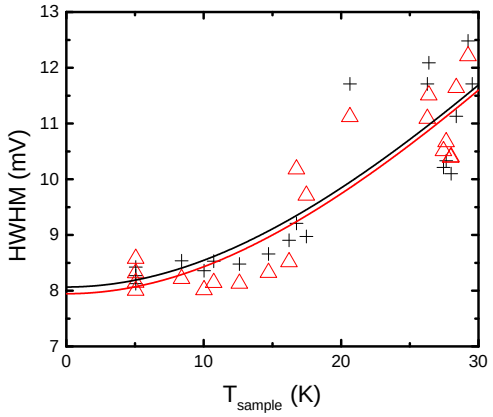

FIG. 4. (Color online)(a) Temperature dependence of the half width at half maximum (HWHM) of the Kondo resonance: The black crosses show the experimental data and the red triangles the background subtracted data. The continuous lines show the corresponding fits to the theoretically predicted temperature dependence (see ref. [16]). 2 HWHM=$\sqrt{(\alpha k_B T)^2 + (2k_B T_K)^2}$. From theory, α should be 2π, which is in good agreement with $\alpha = 6.55$ and 6.54 found here for original and background subtracted data, respectively.

temperature dependence is negligible. Such measurements have been limited to T=35 K by the increasing diffusion of the molecules on the surface. The width of the resonance follows the expected temperature dependence [19], thus confirming that the observed peak is indeed a Kondo resonance [19, 20].

STS spectra taken at various positions on the molecule show different Fano line shapes, corresponding to a strongly deviating asymmetry parameter q. In Fig. 3(b) two examples with different line shapes are shown. To emphasize the asymmetry, the linear and constant terms in equation (1) were subtracted and the resulting functions normalized. As one can see in Fig. 3(b), the asymmetry factor q of the resonance changes in sign over a distance of less than 3 Å. Between these two points, the resonance assumes the form of a symmetric Lorentzian (not shown). Due to the line shape of the Fano function, this symmetric peak in the dI/dV is fitted by very high q values, leading to a pole in the spatial dependence of the asymmetry factor. A smooth change of the sign of q is only possible for dip-like spectra, because for $q = 0$ the Fano function has the shape of an inverted Lorentzian [21].

To obtain a spatial map of the Kondo resonance, we measured a grid of 128 x 128 spectra on the area shown in the inset of Fig. 3 (25 Å x 25 Å) (mesh size of 0.2 Å). We excluded

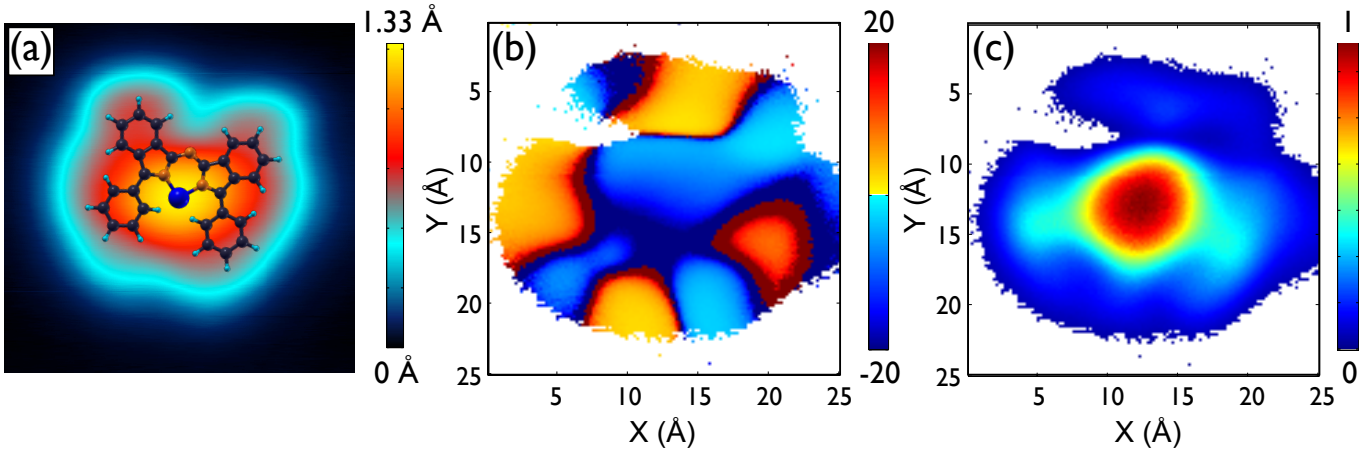

FIG. 5. (Color online)(a) STM topography image with superimposed molecular structure; (b) Spatial distribution of the asymmetry factor q for the same area; (c) Kondo amplitude A. The size of all images is 25 Å x 25 Å. The molecular structure superposed to (a) can be also applied to (b) and (c).

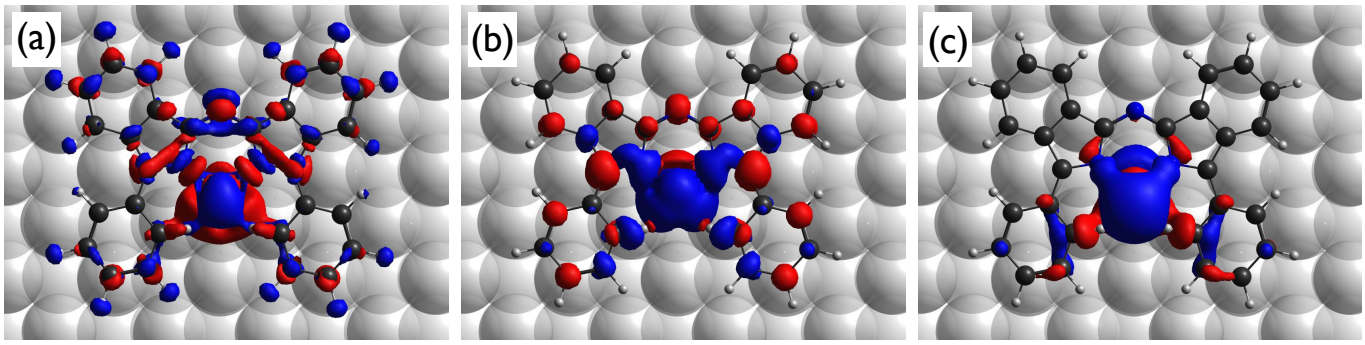

FIG. 6. (Color online)(a) Charge transfer density, (b) spin density, and (c) Kondo active projected molecular orbital. Red indicates positive values, blue negative values.

spectra where the amplitude of the Kondo resonance was less than 4 % of the amplitude at the Co site from the fitting procedure.

In Fig. 5, maps of the asymmetry parameter q (b) and the Kondo amplitude A (c) are compared to the corresponding topography image (a). The structure of the molecule is superimposed on the topography image in Fig. 5(a). The Kondo amplitude A was determined from q and a as proposed by Knorr *et al.* [22]: $A = a \times (1 + q^2)$.

In Fig. 5(c) the Kondo amplitude, while being mainly localized at the Co atom [23], is shown to significantly extend further across the substrate than the molecule itself. The

influence of the organic ligand can be clearly observed in the non-radial symmetry of the Kondo amplitude around the Co atom and the changes in the asymmetry factor q. Moreover, the Kondo resonance is far more prominent on the bis(phenyl) group (lower aromatic rings in Fig. 5(a)) of the Co-BiPADI than on the diisoindole group (upper aromatic rings in Fig. 5(a)).

As one can see in Fig. 5(b), the sign of the asymmetry factor q changes across the molecule (positive values in red, negative values in blue). Interestingly, the contour lines of the two domains with opposite sign correspond to structural features of the organic ligand, although the sign of q changes at the very edge or even next to the Co-BiPADI. The same spatial distribution of the q factor has been observed for all measured molecules. We note that when the molecule is in close proximity to other Kondo-active molecules, slight changes are observed indicating an interaction between neighboring molecules and spins.

According to theory [10, 16], the proportionality factor a and the asymmetry factor q in equation (1) depend on the position $\mathbf{r}$ of the tip. The proportionality factor $a(\mathbf{r})$ is expressed as written below, with the index s numbering, in our case, all hybridized substrate and molecular states, except for the one Kondo state,

$$a(\mathbf{r}) = \frac{4e^2}{\hbar}\rho_{tip}\pi\Sigma_s|V_{st}(\mathbf{r})|^2 V_{Ks}\delta(eV-\epsilon_s) \tag{2}$$

and the asymmetry factor q is expressed as

$$q(\mathbf{r}) = \frac{V_{Kt}(\mathbf{r}) + \Sigma_s V_{st}(\mathbf{r})V_{Ks}P(\frac{1}{eV-\epsilon_s})}{\pi\Sigma_s V_{st}(\mathbf{r})V_{Ks}\delta(eV-\epsilon_s)}. \tag{3}$$

The position dependence in the dI/dV signal is thus traced down to the spatial dependence of the Kondo-orbital/tip matrix element $V_{Kt}(\mathbf{r})$ and the substrate/tip matrix element $V_{st}(\mathbf{r})$.

The first addend in the numerator in equation (3) describes the tunneling directly from the tip into the Kondo state and the second addend represents the tunneling into the substrate with subsequent transfer to the Kondo state. In general, the second addend is considerably smaller then the first one. The denominator is determined by the direct tunneling into the substrate. This interpretation for the asymmetry factor is consistent with the low q values of atomic adsorbates directly on metal substrates [11, 24, 25]. The electrons tunnel predominantly into the continuum of the host metal's conduction band, because of the low extension of the d- or f-states of the impurities into the tunneling gap [16]. Higher q values are found for increased tunneling directly into the magnetic atom [26]. One way to increase

the accessibility of the d- or f-states of the magnetic impurities compared to the states of the supporting metal host is to incorporate the metal atom into an organic ligand [16]. In this way, the magnetic atom is lifted from the surface and the larger coupling between tip and Kondo state V_{Kt} relative to V_{st} can explain the large value of q, but not the pole in its spatial dependence or the change of its sign.

To investigate in detail the electronic properties of our molecule-substrate system, we performed further *ab initio* studies using the Kohn-Sham Hamiltonians obtained from DFT as implemented in the Quikstep module of the CP2K package [27]. Within the energy functional, we use the Goedecker, Teter, and Hutter (GTH) approximation of the pseudoptentials [28, 29]. To approximate the exchange-correlation energy, the meta-generalized gradient approximation (GGA) of Perdue, Burke, and Ernzerhof (PBE) [30] was used. In order to express the system Hamiltonian in the local atomic orbital representation, we used a double-ζ valence basis set plus the polarization functions. In Fig. 6(a,b) the results of spin-dependent DFT images for charge transfer density ($\Delta\rho = \rho_{AgCoBP} - \rho_{Ag} - \rho_{CoBP}$) and spin density are shown. Together with the Bader analysis, which shows some average electron transfer to the molecule, we conclude that the Kondo state is formed by the Co d-orbital hybridized with the ligand orbitals, forming a d_{z^2} orbital as shown in Fig. 6(c). As expected, such d_{z^2} hybridized Co d-state is occupied by one electron according to DFT simulations. Additionally, two other molecular orbitals are close to the Fermi energy of Ag and are also partially occupied due to the finite coupling of these orbitals to the metal states, and there is some polarization over the whole molecule. However, the unpaired spins on the ligand do not show any Kondo resonance because the coupling to the substrate is stronger and the Coulomb interaction is weaker in the case of more extended molecular orbitals.

To go deeper inside the Kondo physics, we performed a localized molecular orbital analysis as was recently suggested in [31]. First, we find localized molecular orbitals at Co-BiPADI and then extend the analysis beyond [31], performing the diagonalization of the Co-BiPADI LMO Hamiltonian. As a result, we obtain *projected molecular orbitals* which represent the result of hybridization between Co-BiPADI and the Ag substrate. Now we can compare the shape of this d_{z^2} hybridized d-orbital (see Fig. 6(c)) to the Kondo amplitude known from experiments (see Fig. 5(c)). Both show the same spatial dependence. The spin polarization (Fig. 6(b)) cannot be experimentally observed. This is attributed to how fast the spin flip exchange processes are, compared to the long acquisition time of dI/dVspectra. Hence, the

different polarities are averaged over time in the STS measurements.

Based on the comparison of our experimental and theoretical results, we conclude that the changing sign of q can be explained by the change of sign of the substrate/tip matrix element $V_{st}(\mathbf{r})$. The Kondo-orbital/tip matrix element $V_{Kt}(\mathbf{r})$ at the same time stays small and smooth, because it is determined mainly by tunneling to the localized orbital in the central part of the molecule. This conclusion is directly supported by the picture of the Kondo amplitude spatial dependence presented in Fig. 5(c). Indeed, at large q (which is the case near the boundary) the amplitude is approximately proportional to the Kondo-orbital/tip coupling

$$A = a(1 + q^2) \propto |V_{Kt}(\mathbf{r})|^2, \tag{4}$$

and does not show any special behavior across the molecule edge. As a possible reason for the sign change of $V_{st}(\mathbf{r})$, we suggest the interference of substrate electron states at the molecule [32]. The onset of this projected bulk state was measured at considerably higher bias, but due to changes of the electronic surface properties near the molecular adsorbate it could be influencing the electronic states near the Fermi level [33]. We note that the spatial dependence of q follows the position of the phenyl rings of the molecule, like those seen for the interference patterns of surface state free electrons in the presence of molecular adsorbates [34]. The periodic changes of the surface electronic states caused by the Ag bulk states projected onto the (100) surface thus influence the value of q via the substrate/tip matrix element $V_{st}(\mathbf{r})$ (see equation (3)). Accordingly, the sign of q would also change in the direction of the π-electronic side groups of the ligand, but the decay length of the resonance is too short compared to the periodicity of the surface oscillation to measure this effect.

In conclusion, the line shape and the amplitude of the Kondo resonance of Co-BiPADI spatially varies and is clearly related to the structure of the organic ligand. The Kondo resonance is mainly localized at the Co atom, but extends non-radially more than 10 Å away from the central atom. Moreover, the asymmetry factor q is strongly influenced by the presence of the molecular ligand. The sign of the q factor changes in close proximity to the molecule, suggesting the influence of the modified substrate's electronic structure near the molecular adsorbate. The pronounced extension of the Kondo amplitude in certain directions underlines the importance of the structure of organic ligands for the coupling of molecular Kondo-systems. This phenomenon could even have a potential application as a tool to mediate direction dependent coupling in future Kondo lattices.

ACKNOWLEDGMENTS

Fruitful discussions with Mathias Voijta, Felix Zörgiebel, Thomas Brumme, Melanie Lorenz, and Moritz Riede are gratefully acknowledged. We gratefully acknowledge support from the German Excellence Initiative via the Cluster of Excellence EXC 1056 "Center for Advancing Electronics Dresden" (cfaed). Funding by the European Union via the ICT-FET Integrated Project PAMS and the Deutsche Forschungsgemeinschaft/National Science Foundation project NSF 11-568, and the International Helmholtz Research School Nanonet is gratefully acknowledged. GC acknowledges support from the "Harmonia" project. Computational facilities were provided by the Zentrum für Informationsdienste und Hochleistungsrechnen (ZIH) in TU Dresden.

[1] U. G. E. Perera, H. J. Kulik, V. Iancu, L. G. G. V. Dias da Silva, S. E. Ulloa, N. Marzari, and S.-W. Hla, Phys. Rev. Lett. **105**, 106601 (2010).

[2] D. Wegner, R. Yamachika, X. Zhang, Y. Wang, T. Baruah, M. R. Pederson, B. M. Bartlett, J. R. Long, and M. F. Crommie, Phys. Rev. Lett. **103**, 087205 (2009).

[3] I. Fernández-Torrente, K. J. Franke, and J. I. Pascual, Phys. Rev. Lett. **101**, 217203 (2008).

[4] A. Zhao, Q. Li, L. Chen, H. Xiang, W. Wang, S. Pan, B. Wang, X. Xiao, J. Yang, J. G. Hou, and Q. Zhu, Science **309**, 1542 (2005).

[5] S. Mülleger, M. Rashidi, M. Fattinger, and R. Koch, J. Phys. Chem. C **117**, 5718 (2013).

[6] J. Kügel, M. Karolak, J. Senkpiel, P.-J. Hsu, G. Sangiovanni, and M. Bode, Nano Lett. **14**, 3895 (2014).

[7] J. Kügel, M. Karolak, A. Krönlein, J. Senkpiel, P.-J. Hsu, G. Sangiovanni, and M. Bode, Phys. Rev. B **91**, 235130 (2015).

[8] Y.-h. Zhang, S. Kahle, T. Herden, C. Stroh, M. Mayor, U. Schlickum, M. Ternes, P. Wahl, and K. Kern, Nat. Commun. **4**, 3110 (2013).

[9] N. Tsukahara, S. Shiraki, S. Itou, N. Ohta, N. Takagi, and M. Kawai, Phys. Rev. Lett. **106**, 187201 (2011).

[10] V. Madhavan, W. Chen, T. Jamneala, M. F. Crommie, and N. S. Wingreen, Phys. Rev. B **64**, 165412 (2001).

[11] J. Li, W.-D. Schneider, R. Berndt, and B. Delley, Phys. Rev. Lett. **80**, 2893 (1998).

[12] H. Prüser, M. Wenderoth, P. E. Dargel, A. Weismann, R. Peters, T. Pruschke, and R. G. Ulbrich, Nat. Phys. **7**, 203 (2011).

[13] H. Prüser, M. Wenderoth, A. Weismann, and R. G. Ulbrich, Phys. Rev. Lett. **108**, 166604 (2012).

[14] S. Meierott, N. Néel, and J. Kröger, Phys. Rev. B **91**, 201111 (2015).

[15] J. M. Soler, E. Artacho, J. D. Gale, A. Garca, J. Junquera, P. Ordejn, and D. Snchez-Portal, Journal of Physics: Condensed Matter **14**, 2745 (2002).

[16] M. Ternes, A. J. Heinrich, and W.-D. Schneider, J. Phys.: Condens. Matter **21**, 053001 (2009).

[17] P. Wahl, L. Diekhöner, M. A. Schneider, and K. Kern, Rev. Sci. Instrum. **79**, 043104 (2008).

[18] P. Wahl, L. Diekhöner, M. A. Schneider, L. Vitali, G. Wittich, and K. Kern, Phys. Rev. Lett. **93**, 176603 (2004).

[19] K. Nagaoka, T. Jamneala, M. Grobis, and M. F. Crommie, Phys. Rev. Lett. **88**, 077205 (2002).

[20] A. F. Otte, M. Ternes, K. von Bergmann, S. Loth, H. Brune, C. P. Lutz, C. F. Hirjibehedin, and A. J. Heinrich, Nat. Phys. **4**, 847 (2008).

[21] M. Plihal and J. W. Gadzuk, Phys. Rev. B **63**, 085404 (2001).

[22] N. Knorr, M. A. Schneider, L. Diekhöner, P. Wahl, and K. Kern, Phys. Rev. Lett. **88**, 096804 (2002).

[23] M. Romero and A. A. Aligia, Phys. Rev. B **83**, 155423 (2011).

[24] V. Madhavan, W. Chen, T. Jamneala, M. F. Crommie, and N. S. Wingreen, Science **280**, 567 (1998).

[25] W. Chen, T. Jamneala, V. Madhavan, and M. F. Crommie, Phys. Rev. B **60**, R8529 (1999).

[26] A. J. Heinrich, J. A. Gupta, C. P. Lutz, and D. M. Eigler, Science **306**, 466 (2004).

[27] J. VandeVondele, M. Krack, F. Mohamed, M. Parrinello, T. Chassaing, and J. Hutter, Comput. Phys. Commun. **167**, 103 (2005).

[28] S. Goedecker, M. Teter, and J. Hutter, Phys. Rev. B **54**, 1703 (1996).

[29] C. Hartwigsen, S. Goedecker, and J. Hutter, Phys. Rev. B **58**, 3641 (1998).

[30] J. P. Perdew, K. Burke, and M. Ernzerhof, Phys. Rev. Lett. **77**, 3865 (1996).

[31] D. A. Ryndyk, A. Donarini, M. Grifoni, and K. Richter, Phys. Rev. B **88**, 085404 (2013).

[32] R. Ohmann, C. Toher, J. Meyer, A. Nickel, F. Moresco, and G. Cuniberti, Phys. Rev. B **89**, 205433 (2014).

[33] L. Vitali, G. Levita, R. Ohmann, A. Comisso, A. De Vita, and K. Kern, Nat. Mater. **9**, 320 (2010).

[34] F. Moresco, L. Gross, M. Alemani, K.-H. Rieder, H. Tang, A. Gourdon, and C. Joachim, Phys. Rev. Lett. **91**, 036601 (2003).